Biomechanical response of the maxillofacial skeleton to transpalatal orthopedic force in a unilateral palatal cleft

Pawan Gautam[a]; Linping Zhao[b]; Pravin Patel[c]

ABSTRACT

Objectives: To assess the skeletal and dental effects of rapid maxillary expansion in a patient with unilateral cleft deformity of secondary palate and alveolus using the finite element method.

Materials and Methods: A patient-specific composite skull model was developed from a patient computed tomographic scan and a surface scan of the patient's maxillary cast using MIMICS imaging analysis software. For volumetric meshing and the finite element analysis, Abaqus (6.7) was used.

Results: The typical wedge-shaped opening that occurs after RME, seen in non-cleft patients, is not seen in cleft patients. A clockwise rotation of the maxilla as a result of maxillary expansion was evident. The areas of maximum stress were the intact primary palate region, inferior orbital foramen of the non-cleft and the cleft sides, and the zygomatic buttress of the cleft side. During expansion, the intact primary palate showed high stress and acted as a region of major resistance, followed by the zygomatic buttress on the cleft side.

Conclusions: Clinicians should consider a need for customization of expansion therapy for cleft patients depending on the patient's age, the type of cleft present (primary or secondary palate), and the desired area of expansion (anterior or posterior). (*Angle Orthod.* 2011;81:503–509.)

KEY WORDS: Rapid maxillary expansion; Cleft palate; FEM

INTRODUCTION

Unilateral cleft palate patients (CLPs) frequently present with an asymmetric maxillary transverse deficiency with collapsed lateral segment on the cleft side. As a consequence, rapid maxillary expansion (RME) is commonly used as part of sequential treatment for CLP patients for the correction of the constricted maxillary arch. A number of modalities of RME and surgically assisted RME have been developed to achieve the expansion and to prevent postexpansion relapse.

[a] Postdoctoral, Craniofacial and Skeletal Diseases Branch, NIDCR/NIH, Bethesda, Md.

[b] Research Director, Craniofacial Center (MC 588), University of Illinois at Chicago, Chicago, Ill.

[c] Associate Professor, Craniofacial Surgery, Craniofacial Center (MC 588), University of Illinois at Chicago, Chicago, Ill.

Corresponding author: Dr Pawan Gautam, Craniofacial Center (MC 588), University of Illinois at Chicago, 811 South Paulina Street, Chicago, IL 60612.

The effects of RME on non-CLP patients have been well established both clinically[1] and experimentally using a finite element model (FEM).[2–4] Both clinical[5–7] and FEM[8,9] studies on clefts have shown asymmetric response of the cleft and non-cleft segments with expansion forces. Previous in vitro studies in non-cleft patients have shown that the primary anatomical sites of resistance to expansion forces were the midpalatal area and the zygomatic buttress. Based on their photoelastic analysis, Chaconas and Caputo[10] pointed out that the articulation between the maxilla and the pterygoid plate of the sphenoid bone is the limiting factor, regardless of how much the suture between the two halves of the maxilla is affected by orthopedic forces. With the missing midpalate and anatomical deformity of the maxillary bone in the CLP patient, it can be expected that the interaction mechanism between the expansive force and resistance to expansion would be different in these patients. The response to maxillary expansion in CLP patients could be better understood using the biomechanical stress-strain and displacement response with FEM. By studying the stress-strain distribution, an appropriate surgical technique could be developed for surgically assisted rapid palatal expansion (SARPE), which
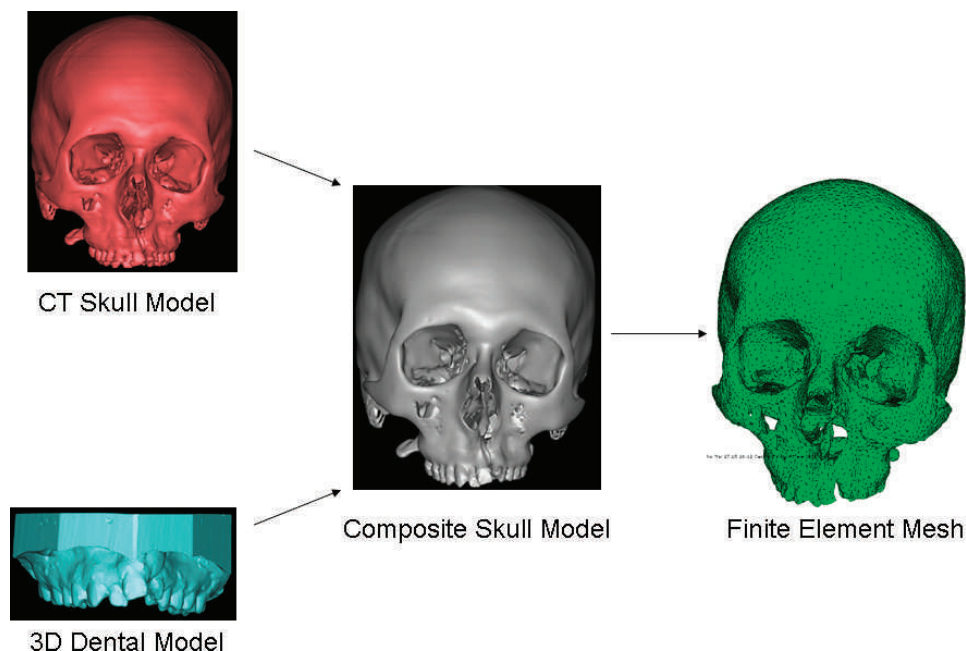
Figure 1. The modeling procedure.

would lead to a predictable and stable response in adults requiring maxillary expansion.

The aim of the present study was to assess the skeletal and dental effects of RME in a patient with unilateral cleft deformity of secondary palate and alveolus using the FEM. This study is a preliminary step in the development of a surgical technique for SARPE, one that is customized for unilateral cleft palate patients using the FEM displacement and stress-strain analysis.

MATERIALS AND METHODS

With institutional review board approval, an archived computed tomographic (CT) scan (slice increment, 0.625; pixel size, 0.488; matrix, 512 × 512 pixels) of a patient with unilateral cleft deformity of secondary palate and alveolus was used in the study. The patient was 16 years old, male, and previously had undergone repair of the lip and palate during infancy, with subsequent alveolar bone graft.

How accurately the FEM simulates the clinical results depends on the how closely the FEM modeling and forces have been simulated. A three-dimensional (3D) composite skull model was used to accurately represent the dental and craniofacial structures (Figure 1). The model of the skull was created using CT scan images of the patient before he underwent RME. To generate the skull model from these CT images, MIMICS (Materialise Inc, Leuven, Belgium) software was used. The CT data are not accurate in generating the 3D models of teeth as a result of artifact.[11,12]

To accurately model the teeth in this study, the maxillary impression was made and poured with dental stone. The stone model was then scanned using the 3D laser scanner (LPX 1200 Roland Laser Scanner, Roland DGA Corporation, Irvine, Calif). The 3D model of the maxillary cast was imported as an STL file in the MIMICS (Materialise) software. The maxillary crowns from the skull model were sectioned and replaced with maxillary dentition derived from the 3D cast. The composite skull model thus generated was exported and meshed using Abaqus (6.7) (SIMULIA, Providence, RI). 3D tetrahedron elements were used for meshing (Figure 1). The present model consisted of 131,029 tetrahedron elements. The volume mesh from Abaqus (6.7) (SIMULIA) was imported to MIMICS (Materialise) to assign the material properties (Table 1).[13] The material properties were assigned to the cortical bone, cancellous bone, and teeth based on the Hounsefield units. For the boundary conditions, a zero displacement and rotation was imposed on nodes around the foramen magnum. To simulate the expansion, the displacement between the node of premolars and molars was simulated with 0.25-mm increments, with total expansion being 2 mm on each side. The biomechanical response of the model was analyzed in terms of Von Mises (VM) stress and displacements.

Table 1. Mechanical Properties Assigned

	Young's Modulus (N/mm²)	Poisson's Ratio
Cortical bone	13,426	0.3
Cancellous	7742	0.3
Teeth	19,600	0.3

Table 2. Displacement Pattern (mm)[a]

	X	Y	Z
ANS	0.16	1.15	−1.46
A′	−0.56	1.06	−1.39
Prosthion	−0.78	1.08	−1.45
Nasal cavity superior	−0.49	0.25	−0.37
Nasal cavity inferior	0.17	1.08	−1.18
Non-cleft side			
Central incisor	−1.19	1.19	−1.82
Canine	−1.45	0.68	−0.59
Second premolar	−1.91	0.32	−0.05
First molar MB cusp	−1.96	0.36	−0.11
Second molar MB cusp	−2.09	0.29	0.11
Maxillary tuberosity	−1.39	0.28	0.29
Lateral nasal wall	0.36	0.95	−0.67
Lateral pterygoid			
Superior	−0.82	0.26	0.42
Inferior	−1.08	0.36	0.21
Medial pterygoid			
Superior	−0.42	0.53	−0.27
Inferior	−1.11	0.52	−0.14
Zygomatic bone			
Frontal process	−0.23	0.06	−0.03
Maxillary process	−0.22	0.06	0.09
Temporal process	−0.27	0.01	0.013
Body	−0.26	−0.01	−0.01
Frontal Pr. maxilla	−0.25	0.41	−0.41
Cleft side			
Canine	0.02	0.36	−0.71
Second premolar	1.36	−0.43	0.15
First molar MB cusp	1.77	−0.51	0.27
Second molar MB cusp	2.19	−0.58	0.34
Maxillary tuberosity	1.44	−0.38	0.18
Lateral nasal wall	−1.42	0.24	−0.52
Lateral pterygoid			
Superior	0.23	−0.08	−0.11
Inferior	1.14	−0.32	0.14
Medial pterygoid			
Superior	0.01	0.09	−0.30
Inferior	1.35	0.08	−0.47
Zygomatic bone			
Frontal process	−0.23	−0.23	−0.04
Maxillary process	−0.27	−0.56	0.09
Temporal process	−0.24	−0.57	−0.26
Body	−0.23	−0.65	0.06
Frontal Pr. maxilla	−0.56	0.23	−0.28

[a] For the non-cleft side, negative X values indicate lateral expansion. For the cleft side, positive X values indicate lateral expansion. Positive Y and Z values denote anterior and superior movement, respectively, on both sides.

RESULTS

Displacement Pattern

The anterior structures of the maxilla moved anteriorly and inferiorly (Table 2). The maximum lateral displacement for maxillary teeth was observed at the second molar, followed by the first molar, second premolar, canine, and central incisor on both cleft and non-cleft sides; therefore, posterior expan-sion was greater compared to the anterior expansion (Figure 2A). In the vertical plane, the separation was pyramidal in shape, with the base of the pyramid located at the oral side of the bone (Figure 2B). The central incisor extrusion was greater compared with that of the second molar on the non-cleft side. On the cleft side, the central incisor moved inferiorly, whereas superior movement of posterior teeth was observed. The tuberosity of the maxilla on the non-cleft side was displaced laterally, anteriorly, and superiorly, while on the cleft side the tuberosity was displaced postero-laterally and superiorly. This indicates clockwise rotation of the maxilla as a result of maxillary expansion. A similar rotational tendency was observed on the cleft side. The lateral bending of the pterygoid plates was evident on both cleft and non-cleft sides. The medial pterygoid plates on both sides moved anteriorly and inferiorly. The lateral pterygoid plates on the non-cleft side moved anteriorly and superiorly. A complex displacement pattern was observed for the lateral pterygoid plates on the cleft side. The zygo-matic bone on the cleft side was displaced postero-medially, whereas zygomatic bone on the non-cleft side was displaced antero-laterally, except for the body of zygomatic bone, which moved postero-laterally. The frontal process of the maxilla on the non-cleft side moved antero-laterally; on the cleft side it was displaced antero-medially.

Stress Pattern

The area of maximum VM stress was the intact primary palate region (Figure 3A); this was followed by the inferior orbital foramen on both sides (Table 3). The zygomatic buttress of the cleft side demonstrated unusually high stress compared to its counterpart on the non-cleft side (Figure 3B). Other areas associated with high VM stress were the medial pterygo-maxillary junction on the cleft side and that on the non-cleft side, in that order. The lateral borders of piriform aperture were also associated with high stresses.

DISCUSSION

A composite skull model was used for FEM analysis. As previous studies[11,12] have shown that CT images are not reliable for generating 3D models of teeth, the 3D laser scanner (Roland DGA Corporation) was used to generate the 3D model of the teeth from the maxillary stone model. The reliability of this scanner in generating 3D models was confirmed in a previous study.[14]

In response to RME, an asymmetric expansion pattern was noted for the two halves of the maxilla. This asymmetric and unpredictable movement of the two halves was also observed for other maxillary
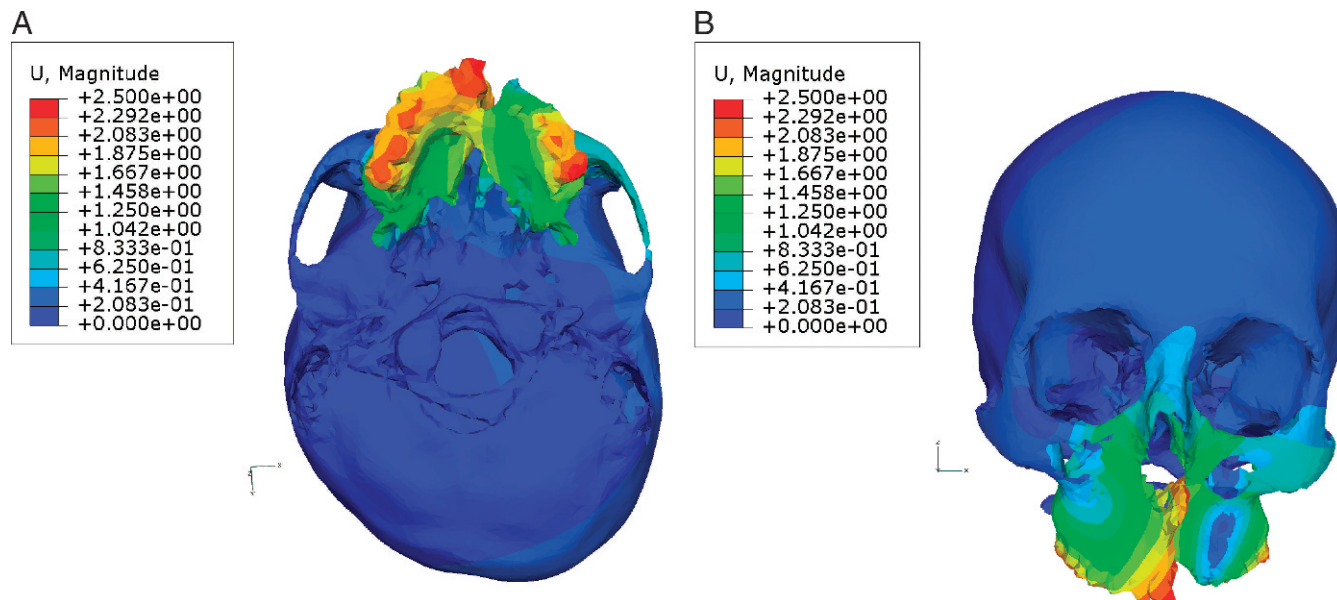
Figure 2. Pattern of displacement with maxillary expansion. (A) Base of the skull view. (B) Frontal view.

articulations, such as the zygomatic and sphenoid bones. This asymmetric response to expansion in unilateral cleft patients has been demonstrated in previous studies.[8,9,15] The expansion was simulated in a patient model with unilateral cleft deformity of the secondary palate and alveolus. The typical wedge-shaped opening in the antero-posterior plane, seen in non-cleft patients, as a result of RME was not seen in the present study. It was observed that the posterior expansion, though asymmetric, was greater compared

to the anterior expansion on both sides. This could be related to the presence of cleft in the secondary palate only. Also, the expansion in the cleft patients occurs in the osseous defects between the premaxilla and the maxilla or at the incisive suture region, rather than at the intra-premaxillary suture, as occurs in normal patients.[15] The intact portion of primary palate on the cleft side showed high stress and acted as a region of major resistance to expansion. The clinical implication of this present finding would be the use of osteotomies
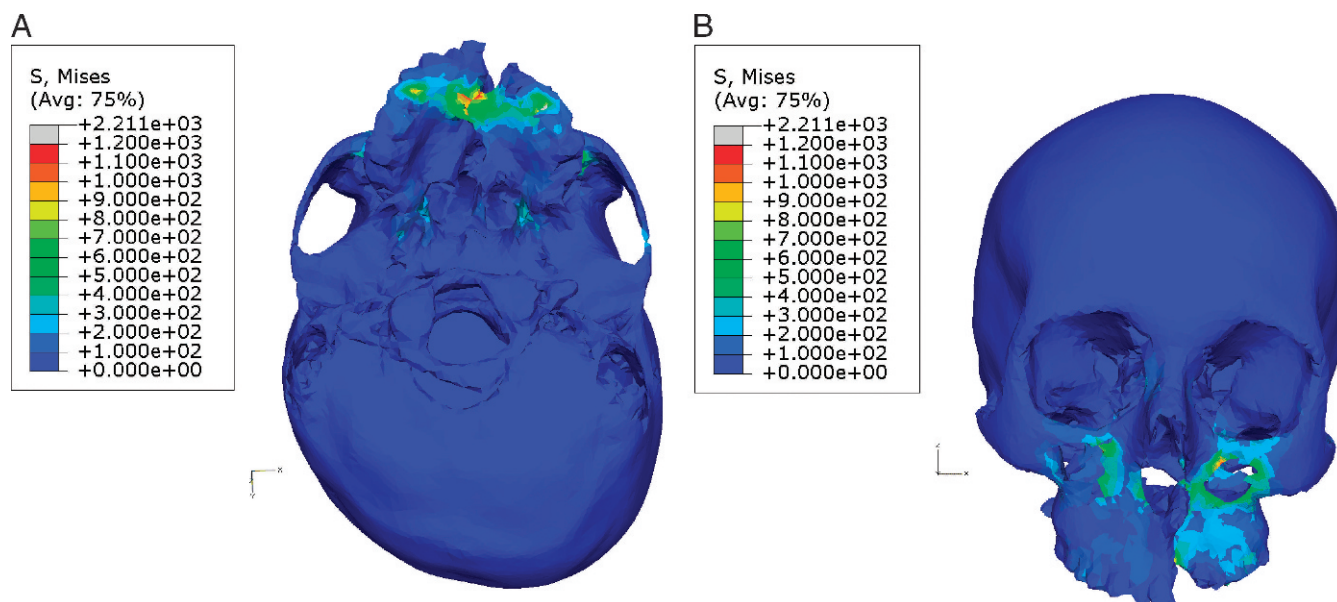

Figure 3. Pattern of Von Mises stress with maxillary expansion. (A) Base of the skull view. (B) Frontal view.

Table 3. Stress Pattern (von Mises Stress) (N/mm²)

Primary palate	1078.9
Nasal cavity (superior)	34.8
Nasal cavity (inferior)	47.5
Fronto-nasal suture	56.4
Non-cleft side	
Inferior orbital rim	150.3
Inferior orbital foramina	695.8
Lateral nasal wall	353.1
Zygomatic buttress	263.8
Lateral pterygoid	
Inferior	5.7
Superior	11.2
Medial pterygoid	
Inferior	23.1
Superior	418.6
Zygomatic bone	
Frontal process	37.4
Maxillary process	180.7
Temporal process	23.7
Body	41.5
Frontal process maxilla	60.9
Maxillary tuberosity	28.8
Pterygo-maxillary junction	
Lateral	119.4
Medial	264.6
Cleft side	
Inferior orbital rim	205.3
Inferior orbital foramina	628.5
Lateral nasal wall	344.4
Zygomatic buttress	621.9
Lateral pterygoid	
Inferior	4.1
Superior	172.1
Medial pterygoid	
Inferior	12.8
Superior	248.6
Zygomatic bone	
Frontal process	59.1
Maxillary process	587.6
Temporal process	39.5
Body	64.8
Frontal process maxilla	29.1
Maxillary tuberosity	30.9
Pterygo-maxillary junction	
Lateral	43.11
Medial	334.1

to separate the two maxillary halves and the simultaneous use of a fan-type expander when expansion is to be carried out in adolescent patients with clefts of the secondary palate and incomplete or intact primary palate. It can be hypothesized that the patients in whom expansion involves the clefts of primary palate will respond differently from those in whom expansion involves the secondary palate cleft (when both are subjected to the same type of expansion therapy). The present study confirmed the clockwise rotation of the

maxilla following RME. This could lead to downward and backward rotation of the mandible. This increased vertical dimension is favorable in most cases of clefts, as overclosure and reduced facial height are common presenting features in patients with clefts.[16]

The naso-maxillary complex and the teeth were displaced anteriorly. Thus, expansion therapy in CLP may have some maxillary protraction effect, which would be beneficial, as maxillary retrusion is a prominent feature of CLP. The lateral displacement of the borders of the piriform aperture clearly demonstrated an increase in nasal cavity width.

The area of the inferior orbital foramina and the zygomatic buttress region demonstrated high stress. This region corresponds to the subtotal LeFort I osteotomy. The zygomatic buttress, particularly on the cleft side, acted as a source of resistance to expansion. This result agrees with the findings of previous studies.[8,9] The medial pterygo-maxillary articulation also showed high stress. The lateral pterygo-maxillary articulation, on the other hand, demonstrated negligible stress.

The surgical component of SARPE normally consists of a subtotal LeFort I osteotomy. Major resistance to expansion in the maxilla seems to be in the maxillary articulations.[17–19] Some authors[20–24] recommend additional palatal osteotomies, while others[19,25] feel that releasing the lateral resistance, such as the zygomatico-maxillary buttress and the maxillary articulations, is sufficient. Additional lateral osteotomies are performed on both sides with separation of the pterygoid plates. Shetty et al.[18] showed the midpalatal suture to be the principal obstruction to maxillary expansion in their experiments on a human photoelastic analogue skull. The present study demonstrated high stress in the midpalatal, zygomatic buttress, lateral border of piriform aperture, and medial pterygo-maxillary junction (in decreasing order). Therefore, in such a case, it would be necessary to perform midpalatal and lateral maxillary buttress osteotomy, which would help in improving the efficiency of SARPE.

Mommaerts[17] demonstrated that during SARPE, pterygo-maxillary disjunction is desired for the posterior expansion, whereas anterior expansion can be carried out without releasing pterygo-maxillary articulation. In our study, the lateral pterygo-maxillary junction offered negligible resistance to expansion, although in this study this resistance could be partly related to the presence of cleft in the secondary palate. The bending of the medial and lateral pterygoid plates was more toward the inferior aspect and was restricted in the superior aspect, close to its cranial articulation. This restriction to lateral bending led to higher VM stress at medial pterygo-maxillary articulations. Hence, the previous findings that connection between the

maxilla and the pterygoid plate of the sphenoid bone (ie, the pterygo-maxillary sutures), regardless of the presence of the midpalate, is one of the sites of major resistance to expansion was partly supported by the present study. In view of this finding, one can argue against the need for lateral pterygo-maxillary dysjunction during SARPE procedure in clefts involving the secondary palate.

On the cleft side, the center of rotation in all three planes of space was located close to the canine region. This was likely a result of the fact that the intact primary palate (close to the canine) acted as a major resistance to expansion. For the non-cleft side, the centers of rotation were located more posteriorly.

Clinical Implications

From the present findings it can be inferred that expansion therapy in clefts patients has to be customized to the patient's individual needs depending on the patient's age, the type of cleft present (primary or secondary palate), and the desired area of expansion (anterior or posterior). In the present study, cleft deformity of the secondary palate and alveolus responded more strongly in the posterior region. It would be interesting to investigate whether patients with complete clefts of the primary palate expand more in the anterior region. It should be kept in mind that our FEM model was derived from a single patient with secondary palate defect and that the skeletal response in clefts of the primary palate was beyond the scope of the present study. In light of the present findings, it can be suggested that in an adolescent patient with unilateral cleft with intact primary palate requiring expansion in the canine region, it would be better to perform SARPE with midpalatal split of the primary palate along with the use of a fan-type expander.

CONCLUSIONS

- The RME led to asymmetric displacement and stress distribution in the two maxillary halves. It can be suggested that the patients with different cleft types may respond differently to the expansion therapy; hence, clinicians should consider the need for customization of expansion therapy for cleft patients depending on the patient's age, the type of cleft present (primary or secondary palate), and the desired area of expansion (anterior or posterior).

REFERENCES

1. Chung CH, Font B. Skeletal and dental changes in the sagittal, vertical, and transverse dimensions after rapid palatal expansion. *Am J Orthod Dentofacial Orthop*. 2004; 126:569–575.

2. Iseri H, Tekkaya AE, Oztan O, Bilgic S. Biomechanical effects of rapid maxillary expansion on the craniofacial skeleton, studied by the finite element method. *Eur J Orthod*. 1998;20:347–356.

3. Jafari A, Shetty KS, Kumar M. Study of stress distribution and displacement of various craniofacial structures following application of transverse orthopedic forces—a three-dimensional FEM study. *Angle Orthod*. 2003;73:12–20.

4. Gautam P, Valiathan A, Adhikari R. Stress and displacement patterns in the craniofacial skeleton with rapid maxillary expansion: a finite element method study. *Am J Orthod Dentofacial Orthop*. 2007;132:5.e1–e11.

5. Subtelny JD, Brodie AG. An analysis of orthodontic expansion in unilateral cleft lip and cleft palate patients. *Am J Orthod*. 1954;40:686–697.

6. Capelozza Filho L, De Almeida AM, Ursi WJ. Rapid maxillary expansion in cleft lip and palate patients. *J Clin Orthod*. 1994;28:34–39.

7. Matthews D. Rapid expansion in clefts. *Plast Reconstr Surg*. 1975;56:396–401.

8. Pan X, Qian Y, Yu J, Wang D, Tang Y, Shen G. Biomechanical effects of rapid palatal expansion on the craniofacial skeleton with cleft palate: a three-dimensional finite element analysis. *Cleft Palate Craniofac J*. 2007;44: 149–154.

9. Holberg C, Holberg N, Schwenzer K, Wichelhaus A, Rudzki-Janson I. Biomechanical analysis of maxillary expansion in CLP patients. *Angle Orthod*. 2007;77:280–287.

10. Chaconas SJ, Caputo AA. Observation of orthopedic force distribution produced by maxillary orthodontic appliances. *Am J Orthod*. 1982;82:492–501.

11. Santler G, Karcher H, Ruda C. Indication and limitations of three-dimensional models in cranio-maxillofacial surgery. *J Cranio-Maxillofac Surg*. 1998;26:11–16.

12. Gateno J, Xia J, Teichgraeber JF, Rosen A. A new technique for the creation of a computerized composite skull model. *J Oral Maxillofac Surg*. 2003;61:222–227.

13. Tanne K, Matsubara S, Sakuda M. Stress distributions in the maxillary complex from orthopedic headgear forces. *Angle Orthod*. 1993;63:111–118.

14. Lee E. *Evaluation of Three Dimensional Digital Data Acquisition Methods for Use in Facial Prosthetic Reconstruction. Biomedical Visualization* [master's thesis]. Chicago, Ill: University of Illinois at Chicago; 2007.

15. Isaacson RJ, Murphy TD. Some effects of rapid maxillary expansion in cleft lip and palate patients. *Angle Orthod*. 1964;34:143–154.

16. Tindlund RS, Rygh P, Bøe OE. Intercanine widening and sagittal effect of maxillary transverse expansion in patients with cleft lip and palate during the deciduous and mixed dentitions. *Cleft Palate Craniofac J*. 1993;30:195–207.

17. Mommaerts MY. Transpalatal distraction as a method of maxillary expansion: technical note. *Br J Oral Maxillofac Surg*. 1999;37:268–272.

18. Shetty V, Mendoca Caridad J, Caputo AA, Chaconas SJ. Biomechanical rationale for surgical-orthodontic expansion of the adult maxilla. *J Oral Maxillofac Surg*. 1994;52: 742–749.

19. Bays RA, Greco JM. Surgically assisted rapid palatal expansion. *J Oral Maxillofac Surg*. 1992;50:110–113.

20. Lehman JA, Haas AJ, Haas DG. Surgical orthodontic correction of transverse maxillary deficiency: a simplified approach. *Plast Reconstr Surg*. 1984;73:62–66.

21. Pogrel MA, Kaban BL, Vargervik K, Baumrind S. Surgically assisted rapid maxillary expansion in adults. *Int J Adult Orthod Orthognath Surg*. 1992;7:37–41.

22. Betts NJ, Vanarsdall RL, Barber HD, Higgins-Barber K, Fonseca RJ. Diagnosis and treatment of transverse maxillary deficiency. *Int J Adult Orthod Orthognath Surg.* 1995;10:75–96.

23. Northway WM, Meade JB. Surgically assisted rapid maxillary expansion: a comparison of technique, response, and stability. *Angle Orthod.* 1997;67:309–320.

24. Turvey TA. Maxillary expansion: a surgical technique based on surgical-orthodontic treatment objectives and anatomical considerations. *J Oral Maxillofac Surg.* 1985;13:51–58.

25. Epker BN, Fish LC. Transverse maxillary deficiency. In: *Dentofacial Deformities: Integrated Orthodontic and Surgical Correction,* Vol 2, 3rd ed. St Louis, Mo: Mosby; 1986: 818–875.